Received: 12 May 2019 | Revised: 21 November 2019 | Accepted: 22 November 2019

DOI: 10.1002/jbm.a.36859

ORIGINAL ARTICLE

3D-engineered GelMA conduit filled with ECM promotes regeneration of peripheral nerve

Hui Gong[1] | Haosheng Fei[1] | Qifan Xu[1] | Maling Gou[2] | Harry H. Chen[1,2]

[1]StemEasy Biotech, Jiangyin, China

[2]Department of Biotherapy, Cancer Center, West China Hospital, Sichuan University, Chengdu, China

Correspondence
Maling Gou, Department of Biotherapy, Cancer Center, West China Hospital, Sichuan University, Chengdu, China.
Email: goumaling@scu.edu.cn
Harry H. Chen, StemEasy Biotech, Jiangyin, Jiangsu, China.
Email: huimin.chen@stemeasy.com

Funding information
the Key Science and Technology Development Plan of Jiangyin, Grant/Award Number: JYKJ3382; Jiangsu Provincial Key Research and Development Program, Grant/Award Number: BE2016010-2

Abstract

Autologous transplantation remains the golden standard for peripheral nerve repair. However, many drawbacks, such as the risk of reoperation or nerve injury remain associated with this method. To date, commercially available artificial nerve conduits comprise hollow tubes. By providing physical guiding and biological cues, tissue engineered conduits are promising for bridging peripheral nerve defects. The present study focuses on the preparation of artificial composite nerve conduits by 3D bio-printing. 3D-printed molds with a tubular cavity were filled with an Engelbreth-Holm-Swarm (EHS) Hydrogel mimicking the extracellular matrix (ECM) basement membrane. Chemically cross-linked gelatin methacryloyl (GelMA) was used to form the conduit backbone, while EHS Hydrogels improved nerve fiber growth while shortening repair time. Statistical significant difference had been found between the blank conduit and the composite conduit group on compound muscle action potential after 4 months. On the other hand, results between the composite conduit group and the autograft group were of no statistical differences. All results above showed that the composite conduit filled with EHS Hydrogel can promote the repair of peripheral nerve and may become a promising way to treat peripheral nerve defects.

KEYWORDS

3D bioprint, chemical cross-link, ECM, GelMA, nerve repair

1 | INTRODUCTION

The incidence of peripheral nerve injury has increased dramatically with the improvement of mechanization in industry and the development of transportation. Every year, peripheral nerve injury accounted for 15–40% of 10–15 million trauma cases arise all over the world (Chen et al., 2015). Microsurgical techniques are now commonly used to repair the end-to-end adventitia of severed peripheral nerve defects and restore their function (Kobayashi, 2018). Autogenous nerve graft or other nerve substitute also represents efficient solutions. However, some drawbacks such as misalignment of nerve bundles, curling of nerve ends, or the proliferation of connective tissue at anastomotic sites still complicate treatments (Nakayama et al., 2007). Biodegradable biomaterials (Senapati, Mahanta, Kumar, & Maiti, 2018) such as poly (L-lactidecoglycolide) (PLGA) (Oh et al., 2008), polyglycolic acid (PGA) (Wang et al., 2005), chitosan (Jiao et al., 2009), silk (Yang et al., 2007), collagen (Archibald, Shefner, Krarup, & Madison, 1995), or gelatin (Chang et al., 2007; Chen et al., 2005, 2006; Lu et al., 2007) are promising compounds. Gelatin can be cross-linked with genipin (Chen et al., 2005) and EDC-NHS (Chang et al., 2007) or under the form of GelMA-LAP (Xia et al., 2018; Zhou, Lee, & Tan, 2017). Noteworthy, Gou and collaborators (Hu et al., 2016) described the use of GelMA and ADSCs to facilitate rat sciatic nerve repair. Here, we report on GelMA conduits filled with an EHS Hydrogel, which contains about 50% laminin and 30% Type IV collagen. During the repair process, the EHS Hydrogel provides a favorable environment supporting the outgrowth of neuron.

2 | MATERIALS AND METHODS

2.1 | Conduit fabrication and characterization

Conduits were produced as described earlier (Hu et al., 2016). Briefly, the mold (Figure 1a,b) was modeled with the use of SolidWorks to create a tubular cavity prior to 3D printing. Based on the size of rat sciatic nerves, the inner and outer diameters were 2 and 4 mm, respectively (Zhao et al., 2016). Five percentage of GelMA (SE-3DP-0200, StemEasy Biotech, China) aqueous solution was prepared at 60°C. After complete dissolution, the solution was cooled to 15°C prior to the addition of 0.5% APS and 0.1% TEMED. The mixture was then poured into the mold and rapidly placed at −20°C. After 24 hr of solidification, the conduit was defrosted and unmolded, followed by intensive rinsing and freeze-drying.

For EHS Hydrogel (SE-EHS-0100, StemEasy Biotech, China) filling, conduits were placed on precooled petri-dishes and 0.1 ml of EHS Hydrogel was poured into the cavity. Conduits were then immediately placed in an incubator. After 5 min, the EHS Hydrogel displayed a jelly-like texture and the composite conduit was considered ready to use.

According to the conventional method, the blank GelMA conduit was examined by scanning electron microscopy (SEM, Phenom ProX, Thermo fisher), and the images were analyzed by ImageJ to calculate the porosity. The blank conduits were immersed in saline in 37°C, and the swelling ratio was calculated by weighing before and after at different time points and calculated by the following formula (Zhao et al., 2016):

$$\text{Swelling ratio} = \frac{\text{wet weight} - \text{dry weight}}{\text{dry weight}} \times 100\%$$

The mechanical properties of GelMA blank conduits were also evaluated by both compression and tensile tests using universal testing systems (5969, Instron, United States) equipped with a 50 N load cell at a rate of 10 m/s. The total length of the samples were 5 mm, tests were lasted until collapsed or flattened.

2.2 | Animals and surgical procedure

All the experiments were conducted following the Institutional Animal Care guidelines with the ethical approval of the West China Hospital Management Committee of Sichuan University. In this experiment, rats weighing 200–300 g were allocated randomly to three groups as followed: the blank conduit group (n = 17), the composite group (n = 15), and the autograft group (n = 15). After anesthesia with 10% chloral hydrate, the skin and muscle of the right lower limb was separated by transverse incision 10 mm sciatic nerve sections were cut out and sutured with the corresponding conduit/nerve. The epineurium of all nerve stumps was sutured to the conduit/nerve four times on each side using 10–0 sutures under a microscope.

2.3 | Gait analysis

At 2, 4, 8, 12, 14, and 16 weeks after the operation, the motor function was evaluated by gait analysis. The toes of experimental side were dipped in ink and the rats were placed on a track (Li et al., 2015). At least four clear footprints were needed to calculate the sciatic function index (SFI) as blow:

$$\text{SFI} = -38.3\,(\text{EPL}-\text{NPL})/\text{NPL} + 109.5(\text{ETS}-\text{NTS})/\text{NTS} + 13.3(\text{EIT}-\text{NIT})/\text{NIT} - 8.8$$

Print length (PL) corresponds to the distance between the third and the heel; toe spread (TS) represents the distance between the first and the fifth toe; intermediary toe spread (IT) corresponds to the distance between the second and the fourth toe. Two datasets were collected: experimental legs (E) and normal legs (N).

2.4 | Electrophysiological evaluation

Electrophysiological tests were performed 4, 6, 8, 10, 12, 14, and 16 weeks following implantation. All animals were analyzed with the use of an electromyograph (Nicolet, United States). After anesthesia, and a stimulation pin was inserted at the proximal end of the graft. The detection pin was plugged into the gastrocnemius muscle and the reference pin was placed in the muscle, near the stimulating pin. The grounding pin was plugged to the tail (Wang, Yang, Wu, Zhang, & Wang, 2017; Wu et al., 2016). Compound muscle action potential (CMAP), nerve conduction velocity (NCV), and latency of CMAP were measured of each rat.

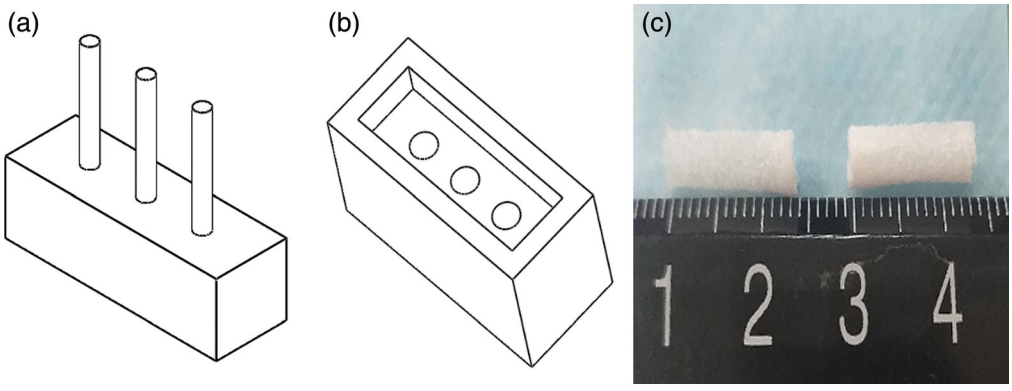

FIGURE 1 Graphical representation of the mold and photographs of the conduits. (a, b) Schematic representation of the conduit mold. (c) Conduits

2.5 | Histological examination

Four, eight, twelve, and sixteen weeks after implantation, the bridging sites of each group were either fixed with 4% formaldehyde and stained with HE or fixed with 5% glutaraldehyde and scanned with a transmission electron microscope JEM1230 (JEOL, Japan). Nerve sections were sampled midway between the proximal and distal ends. For each specimen, more than 20 random axons are analyzed using the Image-J software. In parallel, both sides of the gastrocnemius muscles were harvested and stained with HE.

2.6 | Statistical analysis

All the data were tested in accordance with log-normal distribution. The difference between groups was tested by LSD

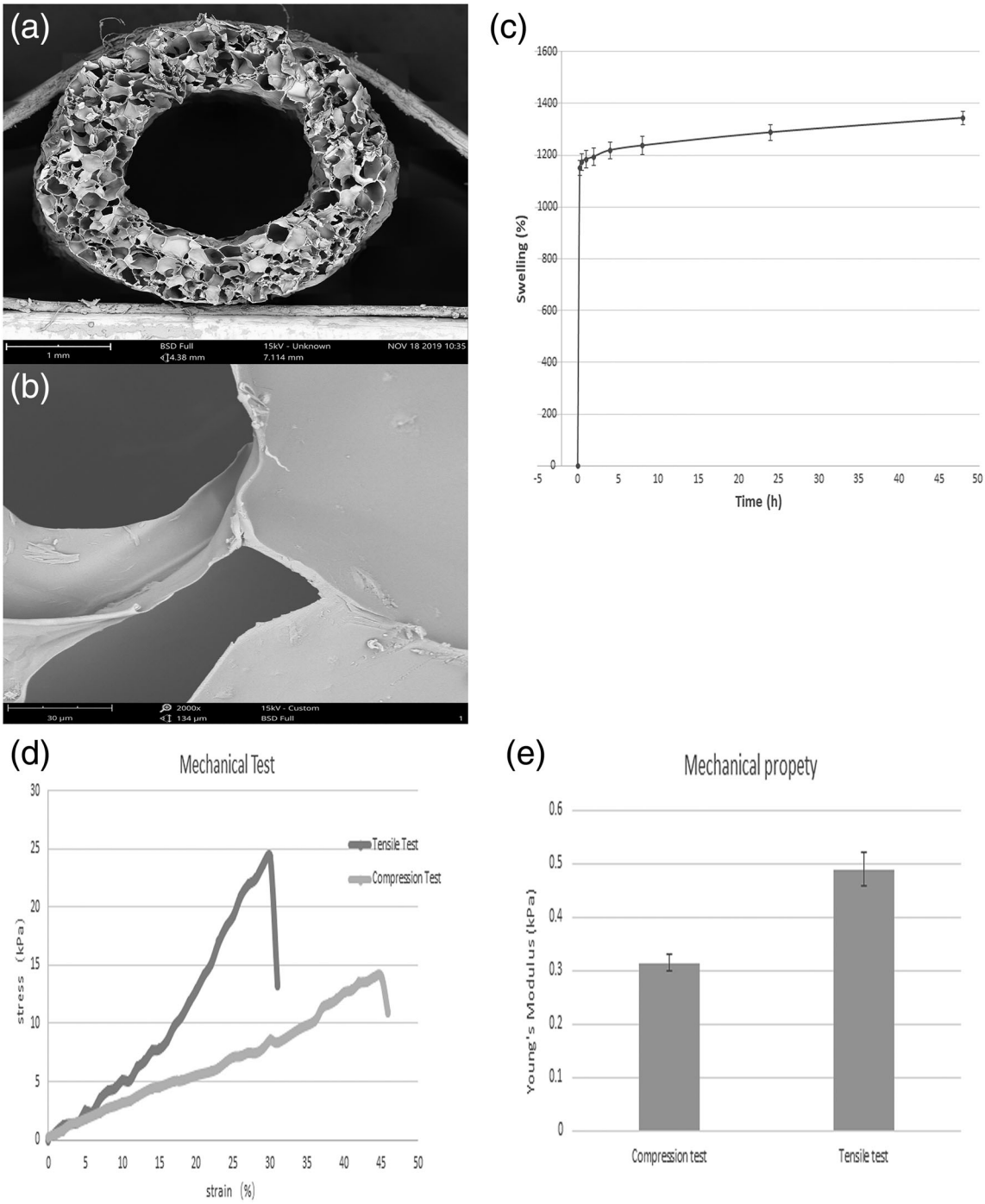

FIGURE 2 Characterization of GelMA conduit. (a) Cross-sectional SEM. (b) Local enlarged SEM. (c) Swelling property. (d) Representative compression/tensile stress–strain curve. (e) Compressive/tensile modulus. GelMA, gelatin methacryloyl; SEM, scanning electron microscopy

afterward. The p value <.05 was considered to have statistical significance.

3 | RESULTS

3.1 | Conduit characterization

All GelMA conduits displayed the same white foamy appearance (Figure 1c) with evenly distributed pores on the wall (Figure 2a,b). According to the data acquired by ImageJ, the porosity was 89.8 ± 0.33% and the pore diameter was 167.6 ± 11.5 μm. In saline, the conduit can reach equilibrium rapidly, and the swelling ratio can reach 1,150 ± 28% just after 5 min, which slowly reached 1,344 ± 27% (Figure 2c). In the mechanical test, the tensile modulus and compression modulus of GelMA conduits (Figure 2d) were 0.489 ± 0.032 kPa and 0.314 ± 0.015 kPa, respectively (Figure 2e).

3.2 | Conduit implantation

Feeding conditions were identical for all rats and each animal was submitted to a daily check for body temperature and stitch cleanliness during 2 weeks following the surgery. No abnormal acute inflammatory response could be observed. The conduits slowly degraded in the blank conduit and composite conduit groups and they completely disappeared after 16 weeks (Figure 3a,b). On the other hand, grafts of the autograft group were stable during the whole experiment (Figure 3c).

3.3 | Walking track analysis

After implantation, all rats experienced walking difficulties. However, surgery did not affect their feeding intake. Rats of the three groups displayed toe swelling, local inflammation, and scab formation to the same extent. The latter were closely monitored and intervention was carried out when appropriate. The SFI illustrates the functional recovery of damaged sciatic nerves. At the beginning (Week 2), SFI showed no difference, with −94.0, −89.9, and −92.8, respectively. SFI values increased during the experiment, indicating that the repair process was similar among groups. Moreover, the composite conduit and the autograft group shared the similar results (Figure 4). Noteworthy, the SFI was still −60.5 high after 16 weeks, indicating that repair was still in progress.

3.4 | Electrophysiological evaluation

Electrophysiological detection is an accepted quantitative indicator of peripheral nerve function recovery. This includes CMAP, NCV, and latency of CMAP. CMAP is related to the number of regenerated motor nerves, while NCV focuses on the speed of conduction of regenerated nerves. Like the SFI, CMAP, and NCV showed a consistent tendency of improvement with time (Figure 5a,b). Differences gradually appeared between the three groups. In particular on CMAP, comparing to the autograft group, significant differences were observed in the blank conduit and composite conduit groups (p < .05) at the time of Week 12. At Weeks 14 and 16, significant differences disappeared between the composite conduit group and the autograft group. On the other hand, the difference between the blank conduit group and the autograft group became obvious (p < .01). At Week 14, NCV was higher in the autograft

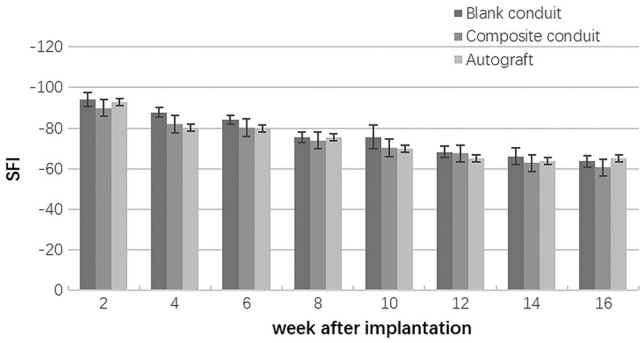

FIGURE 4 SFI of the three group throughout the entire experiment. SFI values varied slightly between the three groups and they increased along the experiment. This indicated a slow but steady repair process. SFI, sciatic function index

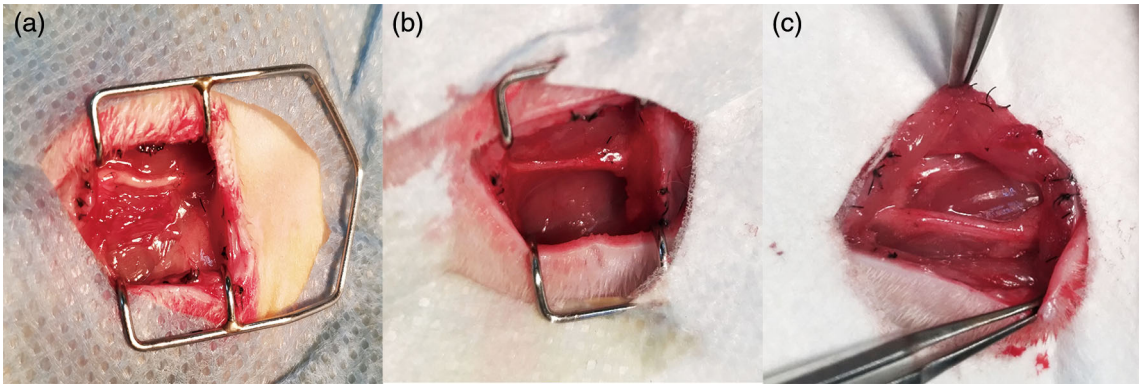

FIGURE 3 Implanted conduit/nerve 16 weeks post-surgery. (a) Blank conduit group. (b) Composite conduit group. (c) Autograft group

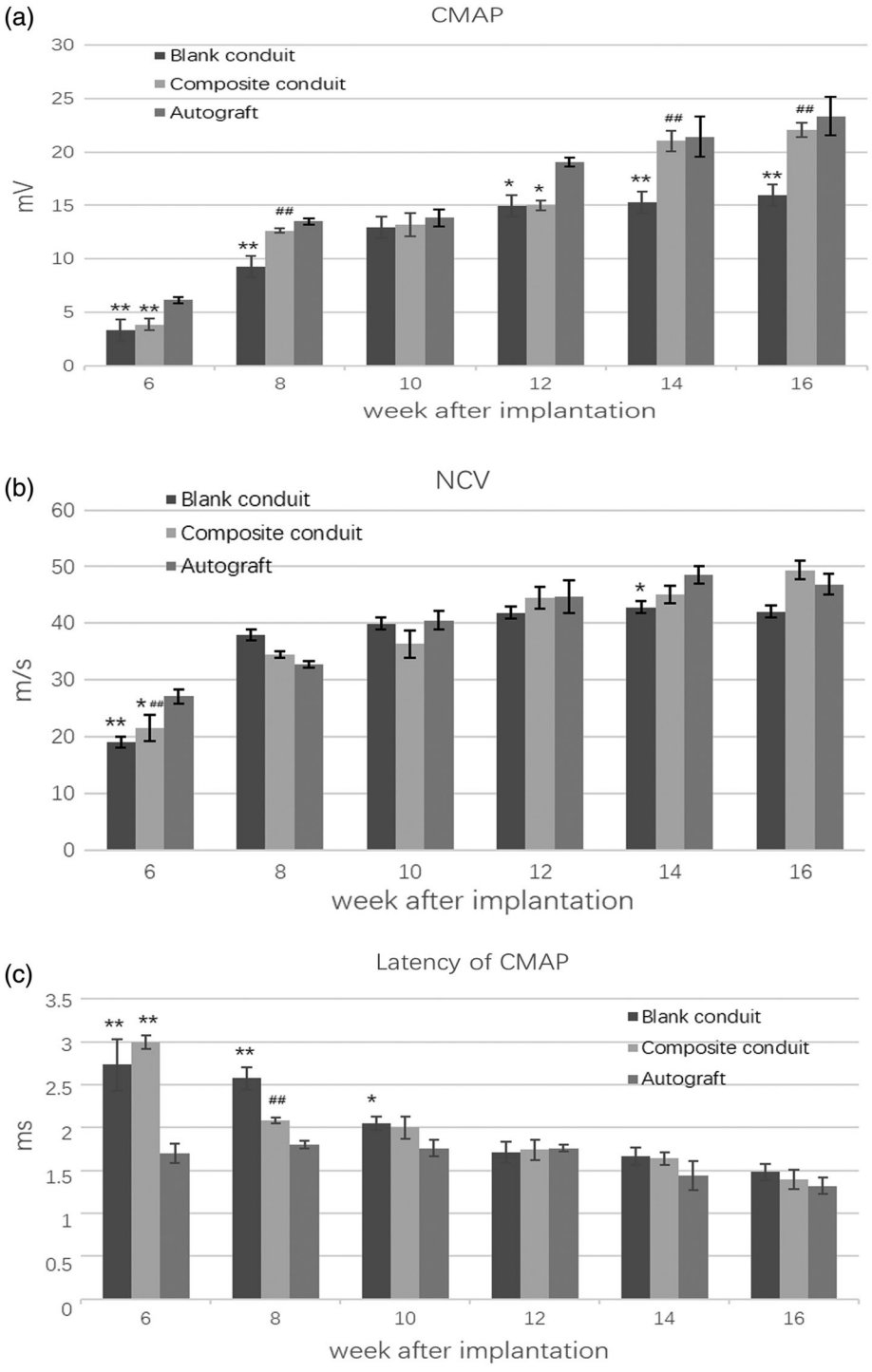

FIGURE 5 Electrophysiological analysis. The CMAP (a), NCV (b), and latency of CMAP (c) were recorded at different time points following surgery. *,** represent comparing to the autograft group while #,## represent comparing to the blank conduit group; *,# mean $p < .05$ and **, ## mean $p < .01$. CMAP, compound muscle action potential; NCV, nerve conduction velocity

group than in the blank conduit group whereas no difference was observed between the composite conduit group and the autograft group ($p < .05$). Latency of CMAP onset decreased over time in all groups and differences disappeared after 12 weeks (Figure 5c).

3.5 | Histological examination

HE staining of gastrocnemius muscle showed that muscle atrophy occurred at Week 12 after nerve defect and repair (Figure 6b,d,f) comparing to health muscle (Figure 6a). Furthermore, the diameter of muscle fibers decreased significantly at Week 16 (Figure 6h) and the gap between muscle fibers became larger (Figure 6c,e,g). At Week 12, differences were significantly among all groups ($p < .01$). Muscle fiber diameter was bigger in the autograft group compared to the composite conduit group. Moreover, it was bigger in the composite group than in the blank conduit group. At Week 16, no difference could be observed between the autograft group and the composite conduit group, in which muscle fibers were significantly bigger than in the blank conduit group (Figure 6h, $p < .01$).

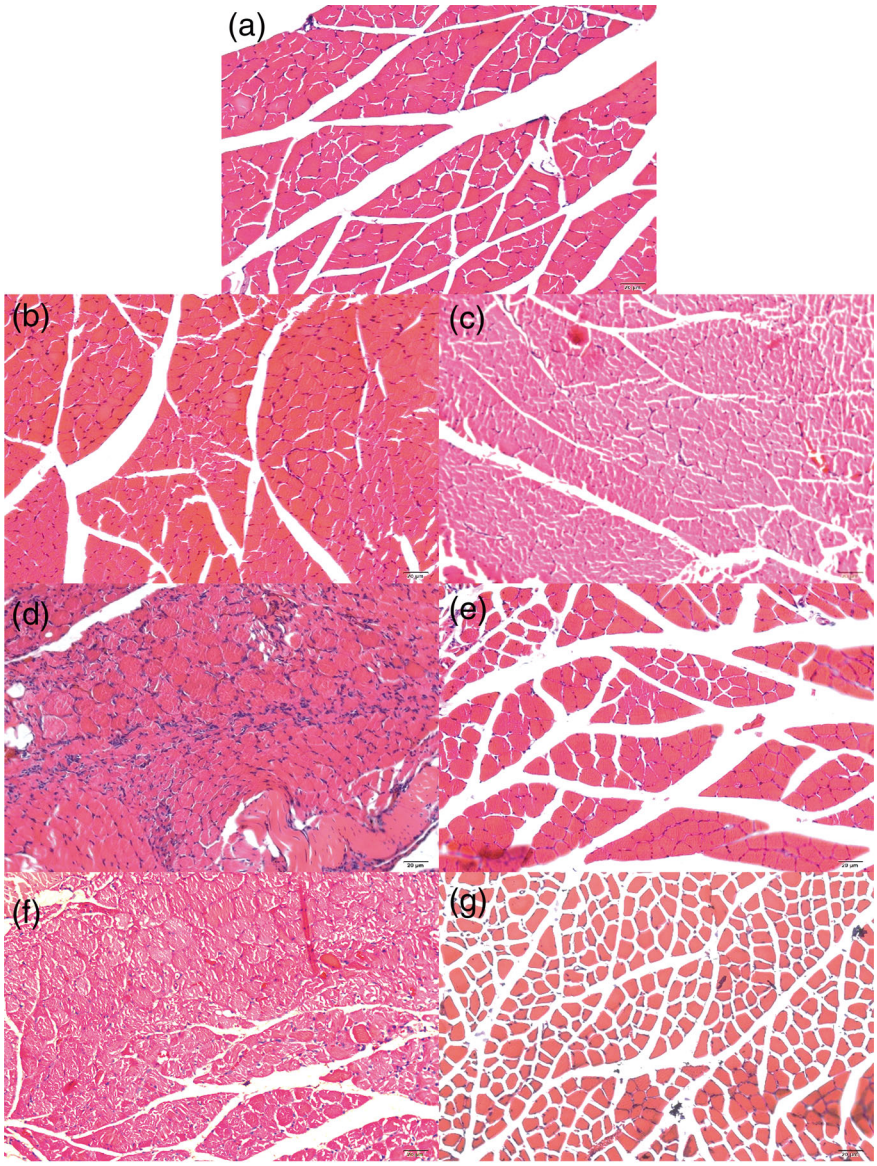

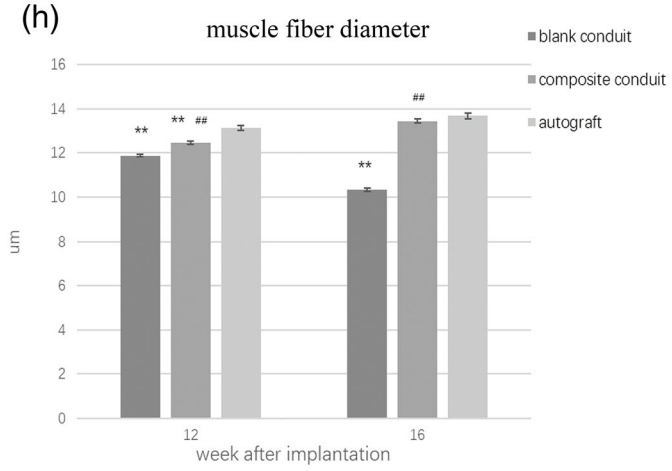

FIGURE 6 HE staining of the gastrocnemius muscle after implantation. (a) Healthy side. (b, c) Blank conduit group at Week 12 (b) and Week 16 (c) after implantation. (d, e) Composite conduit group at Week 12 (d) and Week 16 (e) after implantation. (f, g) Autograft group at Week 12 (f) and Week 16 (g) after implantation. (h) Muscle fiber diameter in the gastrocnemius muscle at Weeks 12 and 16 after implantation. *,** represent comparing to the autograft group while $^{\#}$,$^{\#\#}$ represent comparing to the blank conduit group; *,$^{\#}$ mean $p < .05$ and **, $^{\#\#}$ mean $p < .01$

Transmission electron microscopy at Week 16, showed great morphological differences between the three groups (Figure 7a–c) compared with the contralateral nerve (Figure 7d). The distribution of nerve fibers in the three groups was disordered and nerve fibers were bent and folded. Nerve fiber diameter was statistical different between the composite conduit and autograft groups (Figure 7e). The thickness distribution of myelin sheath was uniform in each group. The three groups had no significant difference (Figure 7f).

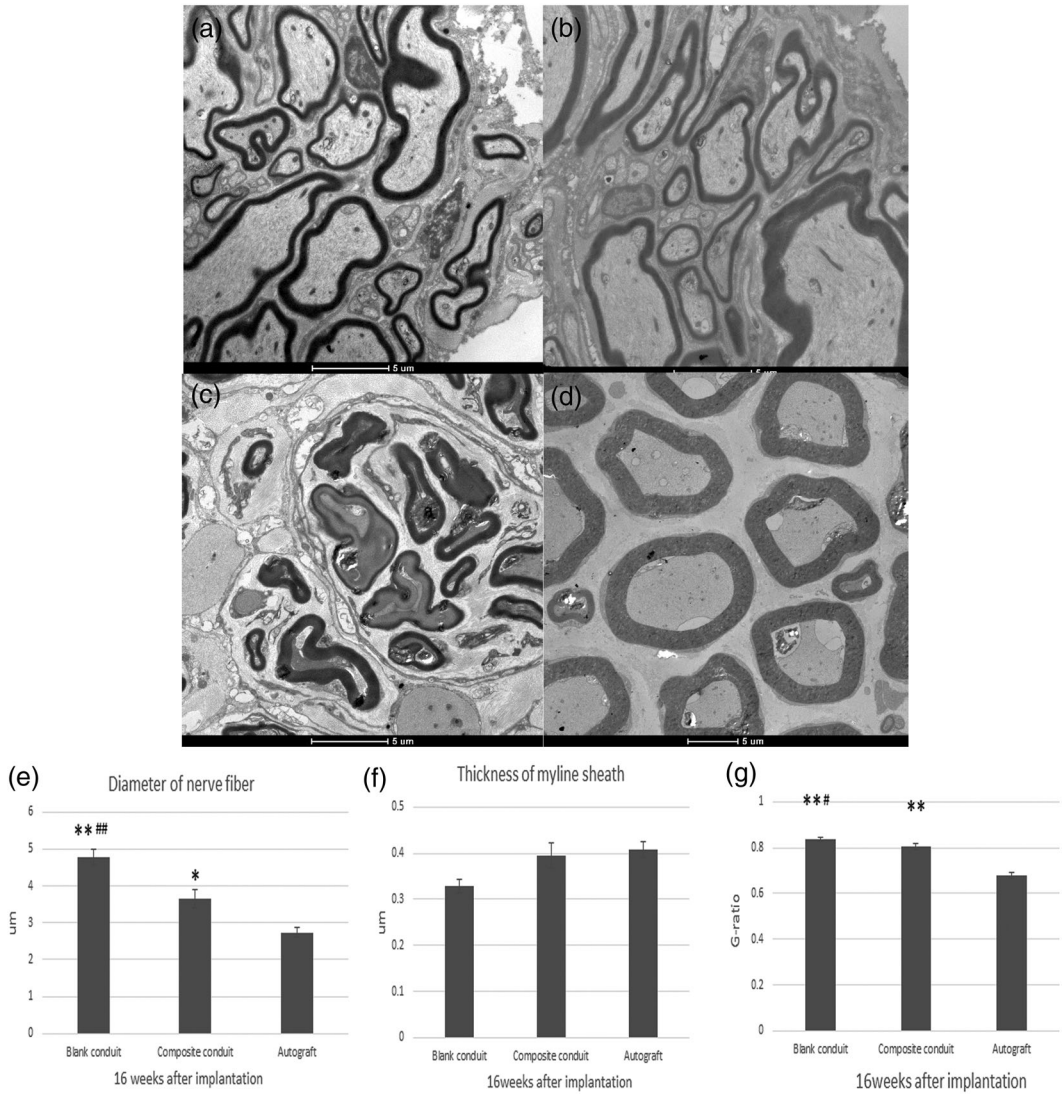

FIGURE 7 Morphological parameters from TEM analysis of regenerated nerves after 16 weeks. (a) Blank conduit group. (b) Composite conduit group. (c) Autograft group. (d) Contralateral nerve. (e) The diameter of nerve fiber. (f) The thickness of myline sheath. *,** represent comparing to the autograft group while $^{\#}$,$^{\#\#}$ represent comparing to the blank conduit group; *,$^{\#}$ mean $p < .05$ and **, $^{\#\#}$ mean $p < .01$. TEM, transmission electron microscopy

There was significant difference in G-ratio among the three groups (Figure 7g).

4 | CONCLUSION AND DISCUSSION

In this study, we implemented a tubular cavity model to prepare nerve conduits. 3D printing was used to precisely control inner and outer diameters and maintain a uniform size along the nerve conduit. GelMA, which can be cured by blue light in the presence of LAP (Lithium phenyl-2,4,6-trimethylbenzoylphosphinate), was chosen for this study. However, we performed chemical cross-link because it ensures uniformity of the pore size, and the material itself displays good biocompatibility. The mechanical strength of chemical cross-linked GelMA were less compared with that of light cured (Chen et al., 2012; Wu et al., 2019), but it is more advantageous in pore size and porosity (Wang et al., 2018). By 3D printing, we can obtain customized nerve conduits, which can provide good scaffold for EHS Hydrogel filling.

The repair efficiency of conduits filling with EHS Hydrogel was carried out on the rat sciatic nerve defect model. Conduits slowly degraded in the blank conduit and composite conduit groups, and it completely disappeared after 16 weeks. SFI, CMAP, NCV, the latency of CMAP and the muscle fiber measurements showed a consistent tendency of improvement with time. Differences between the three groups gradually emerged after 12 weeks. At Week 16 in particular, the composite conduit group and the autograft group showed no significant differences in all test results. Therefore, EHS Hydrogel filling speeds up the repair of nerve defects. This can be explained by the presence of structural proteins such as laminin and collagen IV (Bryan

et al., 2012). Many researchers have applied ECM in peripheral nerve repair using either single components such as laminin (Wang, Hirai, Shimada, Taji, & Zhong, 1992), collagen (Labrador, Butı´, & Navarro, 1998), and so forth or mixed components extracted directly from tissues (Lin et al., 2018; Matsumoto et al., 2000). ECM can be applied alone (Turner, Johnson, Foster, & Badylak, 2018) or filled in conduit (Lin et al., 2018; Matsumoto et al., 2000) as we did. ECM extracted from EHS tissue performed better than blank conduits, alike ECM from porcine urinary bladders (Turner et al., 2018) or porcine decellularized nerve matrix (Matsumoto et al., 2000). Moreover, EHS Hydrogel contained a variety of cytokines (Yang et al., 2003) which could improve nutrition required for nerve repair. It was obvious from histological sections that the myelin sheath, the insulating layer encapsulating nerve fibers, was not thick enough according the G-ratio. Under physiological conditions, the G-ratio of sciatic nerve in rats should be 0.55–0.68 (Chomiak & Hu, 2009), which matched data we got in the contralateral nerve with a value of 0.63. The autograft group showed sufficient myelination with 0.69 G-ratio value, showing the reliability of the operation process, comparing the other two groups with 0.84 and 0.80. It should be noted that the composite conduit group showed more adequate myelination than the blank conduit group. The myelin sheath is composed of Schwann cells and myelin sheath cell membranes. Insufficient myelin sheath thickness, along with thinner never fibers, can cause reduction of conduction velocity (Chomiak & Hu, 2009). Compared with the results from electrophysiology and histology, the results from gait analysis were relatively lagging. Because it has been showed in HE staining that nerve injury leaded to muscle atrophy and may affect the result, meanwhile the synaptic failure leaded to incompetent electrically activation the muscle (Sakuma et al., 2016). It had been reported that gait duty cycle (Johnson et al., 2015) or angle of attack (Yurie et al., 2017) can indicate the functional recovery of sciatic nerve. Gait duty cycle recorded the proportion of the stand time while angle of attack monitored the angle between toe and the metatarsal bone before the paw touch the ground. Both of the methods can enrich the content of function recovery detection.

Many reports described the use of MSC (mesenchyma stem cell)-induced Schwann cells in nerve repair (Kappos et al., 2015; Kingham, Kolar, Novikova, Novikov, & Wiberg, 2014). Studies have found that the function of nerve conduit can be improved in two aspects after differentiated MSC is added, it could either improve axon regeneration and conduit angiogenesis or got better functional performance in SFI and muscle (Kappos et al., 2015). In further studies, the addition of MSC-induced Schwann-like cells directly perfused to pore or cavity of the nerve conduit may improve nerve repair. As a future prospect, we also consider humanizing the EHS Hydrogel with ECM isolated from human placenta in order to facilitate clinical application.

ACKNOWLEDGMENTS

The authors wish to thank the Key Science and Technology Development Plan of Jiangyin (Grant No. JYKJ3382) and Key Research and Development Program of Jiangsu (Grant No. BE2016010) for the financial support.

CONFLICT OF INTEREST

No benefit of any kind will be received either directly or indirectly by the authors.

ORCID

Hui Gong https://orcid.org/0000-0002-5942-2326

REFERENCES

Archibald, S. J., Shefner, J., Krarup, C., & Madison, R. D. (1995). Monkey median nerve repaired by nerve graft or collagen nerve guide tube. *The Journal of Neuroscience*, *15*, 4109–4123.

Bryan, D. J., Litchfield, C. R., Manchio, J. V., Logvinenko, T., Holway, A. H., Austin, J., … Rieger-Christ, K. M. (2012). Spatiotemporal expression profiling of proteins in rat sciatic nerve regeneration using reverse phase protein arrays. *Proteome Science*, *10*, 9.

Chang, J. Y., Lin, J. H., Yao, C. H., Chen, J. H., Lai, T. Y., & Chen, Y. S. (2007). In vivo evaluation of a biodegradable EDC/NHS-cross-linked gelatin peripheral nerve guide conduit material. *Macromolecular Bioscience*, *7*, 500–507.

Chen, M. H., Chen, P. R., Chen, M. H., Hsieh, S. T., Huang, J. S., & Lin, F. H. (2006). An in vivo study of tricalcium phosphate and glutaraldehyde crosslinking gelatin conduits in peripheral nerve repair. *Journal of Biomedical Materials Research. Part B, Applied Biomaterials*, *77B*(1), 89–97.

Chen, S., Chen, Z. G., Dai, H., Ding, J., Guo, J., Han, N., … Zhou, S. L. (2015). Repair, protection and regeneration of peripheral nerve injury. *Neural Regeneration Research*, *10*, 1777–1798.

Chen, Y. C., Lin, R. Z., Qi, H., Yang, Y., Bae, H., Melero-Martin, J. M., & Khademhosseini, A. (2012). Functional human vascular network generated in Photocrosslinkable gelatin methacrylate hydrogels. *Advanced Functional Materials*, *22*, 2027–2039.

Chen, Y.-S., Chang, J.-Y., Cheng, C.-Y., Tsai, F.-J., Yao, C.-H., & Liu, B.-S. (2005). An in vivo evaluation of a biodegradable genipin-cross-linked gelatin peripheral nerve guide conduit material. *Biomaterials*, *26*, 3911–3918.

Chomiak, T., & Hu, B. (2009). What is the optimal value of the g-ratio for myelinated fibers in the rat CNS? A theoretical approach. *PLoS One*, *13*(4), 7754.

Hu, Y., Wu, Y., Gou, Z., Tao, J., Zhang, J., Liu, Q., … Gou, M. (2016). 3D-engineering of cellularized conduits for peripheral nerve regeneration. *Scientific Reports*, *30*(6), 32184.

Jiao, H., Yao, J., Yang, Y., Chen, X., Lin, W., Li, Y., … Wang, X. (2009). Chitosan/polyglycolic acid nerve grafts for axon regeneration from prolonged axotomized neurons to chronically denervated segments. *Biomaterials*, *30*, 5004–5018.

Johnson, B. N., Lancaster, K. Z., Zhen, G., He, J., Gupta, M. K., Kong, Y. L., … McAlpine, M. C. (2015). 3D printed anatomical nerve regeneration pathways. *Advanced Functional Materials*, *25*, 6205–6217.

Kappos, E. A., Engels, P. E., Tremp, M., Meyer zu Schwabedissen, M., di Summa, P., Fischmann, A., … Kalbermatten, D. F. (2015). Peripheral nerve repair: Multimodal comparison of the long-term regenerative potential of adipose tissue-derived cells in a biodegradable conduit. *Stem Cells and Development.*, *24*, 2127–2141.

Kingham, P. J., Kolar, M. K., Novikova, L. N., Novikov, L. N., & Wiberg, M. (2014). Stimulating the neurotrophic and angiogenic properties of human adipose-derived stem cells enhances nerve repair. *Stem Cells and Development.*, *23*, 741–754.

Kobayashi, E. (2018). New trends in translational microsurgery. *Acta Cirúrgica Brasileira*, *33*, 862–867.

Labrador, R. O., Butı´, M., & Navarro, X. (1998). Influence of collagen and laminin gels concentration on nerve regeneration after resection and tube repair. *Experimental Neurology.*, *149*, 243–252.

Li, B., Qiu, T., Iyer, K. S., Yan, Q., Yin, Y., Xie, L., … Li, S. (2015). PRGD/PDLLA conduit potentiates rat sciatic nerve regeneration and the underlying molecular mechanism. *Biomaterials*, *55*, 44–53.

Lin, T., Liu, S., Chen, S., Qiu, S., Rao, Z., Liu, J., et al. (2018). Hydrogel derived from porcine decellularized nerve tissue as a promising biomaterial for repairing peripheral nerve defects. *Acta Biomaterialia*, *73*, 326–338.

Lu, M. C., Hsiang, S. W., Lai, T. Y., Yao, C. H., Lin, L. Y., & Chen, Y. S. (2007). Influence of cross-linking degree of a biodegradable genipin-cross-linked gelatin guide on peripheral nerve regeneration. *Journal of Biomaterials Science. Polymer Edition*, *18*, 843–863.

Matsumoto, K., Ohnishi, K., Kiyotani, T., Sekine, T., Ueda, H., Nakamura, T., … Shimizu, Y. (2000). Peripheral nerve regeneration across an 80-mm gap bridged by a polyglycolic acid (PGA)-collagen tube filled with laminin-coated collagen fibers: A histological and electrophysiological evaluation of regenerated nerves. *Brain Research*, *868*, 315–328.

Nakayama, K., Takakuda, K., Koyama, Y., Itoh, S., Wang, W., Mukai, T., & Shirahama, N. (2007). Enhancement of peripheral nerve regeneration using bioabsorbable polymer tubes packed with fibrin gel. *Artificial Organs*, *31*, 500–508.

Oh, S. H., Kim, J. H., Song, K. S., Jeon, B. H., Yoon, J. H., Seo, T. B., … Lee, J. H. (2008). Peripheral nerve regeneration within an asymmetrically porous PLGA/Pluronic F127 nerve guide conduit. *Biomaterials*, *29*, 1601–1609.

Sakuma, M., Gorski, G., Sheu, S. H., Lee, S., Barrett, L. B., Singh, B., … Woolf, C. J. (2016). Lack of motor recovery after prolonged denervation of the neuromuscular junction is not due to regenerative failure. *The European Journal of Neuroscience*, *43*, 451–462.

Senapati, S., Mahanta, A. K., Kumar, S., & Maiti, P. (2018). Controlled drug delivery vehicles for cancer treatment and their performance. *Signal Transduction and Targeted Therapy*, *3*, 7.

Turner, N. J., Johnson, S. A., Foster, L. J. R., & Badylak, S. F. (2018). Sutureless nerve repair with ECM bioscaffolds and laser-activated chitosan adhesive. *Journal of Biomedical Materials Research. Part B, Applied Biomaterials*, *106*, 1698–1711.

Wang, G., Hirai, K., Shimada, H., Taji, S., & Zhong, S. Z. (1992). Behavior of axons, Schwann cells and perineurial cells in nerve regeneration within transplanted nerve grafts: Effects of anti-laminin and anti-fibronectin antisera. *Brain Research.*, *583*, 216–226.

Wang, G. W., Yang, H., Wu, W. F., Zhang, P., & Wang, J. Y. (2017). Design and optimization of a biodegradable porous zein conduit using microtubes as a guide for rat sciatic nerve defect repair. *Biomaterials*, *131*, 145–159.

Wang, X., Hu, W., Cao, Y., Yao, J., Wu, J., & Gu, X. (2005). Dog sciatic nerve regeneration across a 30-mm defect bridged by a chitosan/PGA artificial nerve graft. *Brain*, *128*, 1897–1910.

Wang, Y., Ma, M., Wang, J., Zhang, W., Lu, W., Gao, Y., … Guo, Y. (2018). Development of a photo-crosslinking, biodegradable GelMA/PEGDA hydrogel for guided bone regeneration materials. *Materials (Basel).*, *11*, E1345.

Wu, R., Wang, L., Chen, F., Huang, Y., Shi, J., Zhu, X., … Zhang, X. (2016). Evaluation of artificial nerve conduit and autografts in peripheral nerve repair in the rat model of sciatic nerve injury. *Neurological Research*, *38* (5), 461–466.

Wu, Y., Xiang, Y., Fang, J., Li, X., Lin, Z., Dai, G., … Zhang, D. (2019). The influence of the stiffness of GelMA substrate on the outgrowth of PC12 cells. *Bioscience Reports*, *18*, 39.

Xia, H., Zhao, D., Zhu, H., Hua, Y., Xiao, K., Xu, Y., … Zhou, G. (2018 Sep 19). Lyophilized scaffolds fabricated from 3D-printed Photocurable natural hydrogel for cartilage regeneration. *ACS Applied Materials & Interfaces*, *10*(37), 31704–31315.

Yang, J. Z., Ho, A. L., Ajonuma, L. C., Lam, S. Y., Tsang, L. L., Tang, N., … Chan, H. C. (2003). Differential effects of Matrigel and its components on functional activity of CFTR and ENaC in mouse endometrial epithelial cells. *Cell Biology International*, *27*, 543–548.

Yang, Y., Ding, F., Wu, J., Hu, W., Liu, W., Liu, J., & Gu, X. (2007). Development and evaluation of silk fibroin-based nerve grafts used for peripheral nerve regeneration. *Biomaterials*, *28*, 5526–5535.

Yurie, H., Ikeguchi, R., Aoyama, T., Kaizawa, Y., Tajino, J., Ito, A., … Matsuda, S. (2017). The efficacy of a scaffold-free bio 3D conduit developed from human fibroblasts on peripheral nerve regeneration in a rat sciatic nerve model. *PLoS One*, *13*, 12.

Zhao, X., Lang, Q., Yildirimer, L., Lin, Z. Y., Cui, W., Annabi, N., … Khademhosseini, A. (2016). photocrosslinkable gelatin hydrogel for epidermal tissue engineering. *Advanced Healthcare Materials*, *5*, 108–118.

Zhou, M., Lee, B. H., & Tan, L. P. (2017). A dual crosslinking strategy to tailor rheological properties of gelatin methacryloyl. *International Journal of Bioprinting*, *3*(2), 130–137.

How to cite this article: Gong H, Fei H, Xu Q, Gou M, Chen HH. 3D-engineered GelMA conduit filled with ECM promotes regeneration of peripheral nerve. *J Biomed Mater Res*. 2019;1–9. https://doi.org/10.1002/jbm.a.36859